Journal of Power Sources 267 (2014) 723–730

Contents lists available at ScienceDirect

Journal of Power Sources

journal homepage: www.elsevier.com/locate/jpowsour

Oxygen ion conduction in barium doped $LaInO_3$ perovskite oxides

Hye-Lim Kim [a], Shin Kim [b], Kyu-Hyung Lee [c], Hong-Lim Lee [a], Ki-Tae Lee [d, e, *]

[a] Department of Materials Science and Engineering, Yonsei University, Seoul 120-749, Republic of Korea
[b] Hasla Co. Ltd, Gangneung 210-340, Republic of Korea
[c] Department of Advanced Materials Science and Engineering, Kangwon National University, Gangwon 200-701, Republic of Korea
[d] Division of Advanced Materials Engineering, Chonbuk National University, Jeonbuk 560-756, Republic of Korea
[e] Hydrogen and Fuel Cell Research Center, Chonbuk National University, Jeonbuk 561-756, Republic of Korea

HIGHLIGHTS

- 3 mol% excess Ba-doped $La_{1-x}Ba_xInO_{3-\delta}$ ($0.4 \leq x \leq 0.8$) is a cubic perovskite structure.
- $La_{1-x}Ba_xInO_{3-\delta}$ ($0.4 \leq x \leq 0.8$) is nearly pure oxygen ion conductor in a dry atmosphere.
- $La_{0.6}Ba_{0.4}InO_{3-\delta}$ exhibited the highest conductivity of 5.6×10^{-2} S cm^{-1} at 800 °C.
- Activation energy was slightly lower than that of the doped $LaGaO_3$ system.

ARTICLE INFO

Article history:
Received 3 April 2014
Received in revised form
2 June 2014
Accepted 2 June 2014
Available online 11 June 2014

Keywords:
Perovskite oxide
Oxygen ion conduction
Conductivity
Tolerance factor
Activation energy

ABSTRACT

Oxygen ion conduction behaviors of the 0–5 mol% excess Ba-doped $La_{0.6}Ba_{0.4}InO_{3-\delta}$ cubic perovskite oxides have been investigated to elucidate their potential as electrolyte materials. The highest conductivity, 5.6×10^{-2} S cm^{-1} at 800 °C, is obtained at the 3 mol% excess Ba-doped composition benefiting from a supplementation of Ba^{2+} ions on the vacant A-site generated by the volatilization during the heat-treatment processes. Interestingly, all the samples except the undoped composition show curved electrical conductivity behavior in the Arrhenius plot. The activation energy is 0.50–0.52 eV in the high-temperature region above 900 °C, which is slightly lower than that of the doped $LaGaO_3$ system. Moreover, all the samples show significantly lower activation energy values of both the high- and low-temperature regions compared with yttria-stabilized zirconia. The 3 mol% excess Ba-doped $La_{1-x}Ba_xInO_{3-\delta}$ ($0.4 \leq x \leq 0.8$) sample has also been studied. All of the compositions show a cubic perovskite structure and a nearly pure oxygen ion conduction behavior in a dry atmosphere even when $p(O_2) = 1$atm. The composition of $x = 0.4$ exhibits the highest oxygen ion conductivities.

1. Introduction

Doped perovskite oxides have come to occupy an important position as ceramic electrolytes for solid oxide fuel cells (SOFCs) because they show high oxygen ion conductivity. Acceptor-doped $LaMO_3$ perovskite oxides (M = Al, Ga, Sc, In, and rare-earth ions) are well known as oxygen ion conductors. Although the oxygen ion conduction of $LaAlO_3$ doped with a rhombohedral structure has been studied widely, the conductivity is too low to be applied as an electrolyte material [1,2]. On the other hand, doped $LaGaO_3$ perovskite oxides have received increasing attention due to their superior oxygen ion conductivity compared to that of yttria-stabilized zirconia (YSZ) with a fluorite structure [3–8]. Oxygen ion conductivity of the Sr and Mg co-doped $LaGaO_3$ is greater than 0.1 S cm^{-1} at 800 °C, which is comparable to that of YSZ at 1000 °C. Indeed, this material is now applied as an electrolyte material for intermediate-temperature SOFCs at 800 °C.

Ba-doped $LaScO_3$ with a cubic structure has been reported as a proton conductor in a wet atmosphere. However, it showed very poor oxygen ion conduction in a dry atmosphere [9,10]. The oxygen ion conductivity of $La_{0.5}Ba_{0.5}ScO_{3-\delta}$ was 4.82×10^{-3} S cm^{-1} at 800 °C. Moreover, scandium oxide is too expensive to be used in industrial products.

For the doped $LaLnO_3$ (Ln = rare-earth ions) with an orthorhombic structure, proton conduction was observed in a wet

* Corresponding author. Division of Advanced Materials Engineering, Chonbuk National University, Jeonbuk 560-756 Republic of Korea. Tel.: +82 63 270 2290; fax: +82 63 270 2386.
E-mail address: ktlee71@jbnu.ac.kr (K.-T. Lee).

http://dx.doi.org/10.1016/j.jpowsour.2014.06.006
0378-7753/

atmosphere, but the oxygen ion conduction was negligible due to the severely distorted structure [11]. In recent studies on doped $LaInO_3$, the Sr-doped compounds with orthorhombic structure showed predominant proton conduction below 600 °C in the presence of water vapor. In particular, Ba and Sr co-doped $LaInO_3$ with a cubic structure showed very high oxygen ion conductivity in a dry atmosphere [12,13]. It has been reported that Ba-doped $LaInO_3$, e.g., $La_{0.6}Ba_{0.4}InO_{3-\delta}$ with a cubic structure, exhibited mixed conduction behavior of oxygen ions and p-type electronic conduction at high oxygen partial pressures under a dry atmosphere, and it became a pure oxygen ion conductor in a N_2 atmosphere [14]. Below 450 °C, it showed proton conduction behavior in a wet atmosphere. Although proton conduction was widely discussed in previous reports, a systematic study of the oxygen ion conduction of Ba-doped $LaInO_3$ has not yet been performed.

Babilo et al. claimed that the A-site deficiency in the yttria-doped $BaZrO_3$ due to barium loss during heat-treatment caused the migration of the dopants from the B-site to the A-site, resulting in a consequent decrease in the unit cell [19]. They also demonstrated the volatilization of Ba in the yttria-doped $BaZrO_3$ during the synthesis process. However, no reports have addressed the volatilization of Ba in Ba-doped $LaInO_3$.

In this study, the effect of Ba content on the oxygen ion conductivity of $La_{0.6}Ba_{0.4}InO_{3-\delta}$ with excess Ba from 0 to 5 mol% has been investigated, and the conduction behavior was discussed with regard to parameters affecting oxygen ion migration. Additionally, the phase formation and the conduction behavior in the $La_{1-x}Ba_xInO_{3-\delta}$ system were investigated.

2. Experimental procedure

For the preparation of undoped and 2–5 mol% excess Ba-doped $La_{0.6}Ba_{0.4}InO_{3-\delta}$, the required amounts of La_2O_3 (High Purity Chem., 99.99%), $BaCO_3$ (High Purity Chem., 99.95%), and In_2O_3 (High Purity Chem., 99.99%) were weighed and then mixed in an alumina mortar for 2 h. Before weighing, La_2O_3 powder was calcined at 1100 °C for 1 h using a box-type furnace and both and $BaCO_3$ and In_2O_3 powders were heated at 200 °C for 24 h in a dry oven in order to remove the absorbed moisture. The mixture of La_2O_3, $BaCO_3$, and In_2O_3 was pressed into a disc and then heated at 1200 °C for 10 h in air. The heat-treated discs were crushed and ground into powder. Heat treatment and grinding was conducted three times for complete homogenization. The resulting powder was uniaxially pressed into discs and isostatically pressed at approximately 138 MPa. Disc-type specimens were then finally sintered at 1500 °C for 10 h in air. For the $La_{1-x}Ba_xInO_{3-\delta}$ system, compositions with 3 mol% excess Ba were prepared.

The phase analysis of the sintered specimen was carried out by a powder X-ray diffraction method using a Rigaku Denki D/MAX RINT 2000 diffractometer with Cu-Kα radiation. Silicon was used as an internal standard material for the measurement of the lattice parameter, and annealing was carried out at 500 °C in a dry N_2 atmosphere using a liquid N_2 trap. The composition of the samples was analyzed by an inductively coupled plasma (ICP) spectrometer. Microstructural characterization was carried out with a Hitachi field emission scanning electron microscope (SEM).

The electrical conductivity was measured in a tube-type furnace by a conventional DC 4-probe method in a dry atmosphere using an ethanol/dry-ice trap. The conductivity measurement was carried out during cooling from 1200 °C. The isothermal conductivity was measured at 800 °C. Oxygen partial pressure, $p(O_2)$, was controlled by use of dry O_2/N_2 mixtures and dry H_2.

3. Results and discussion

3.1. Excess Ba-doped $La_{0.6}Ba_{0.4}InO_{3-\delta}$ system

It has been reported that the contribution of p-type conductivity to the total conductivity for $La_{0.6}Ba_{0.4}InO_{3-\delta}$ under a dry atmosphere was small, that is, $\sigma_{p\text{-type}}/\sigma_{total} = 0.127$ at 800 °C for an oxygen partial pressure of 1 atm, and most of the conducting species in a N_2 atmosphere were oxygen ions ($\sigma_{oxygen\text{-}ion}/\sigma_{total} = 0.985$) [14]. These results indicate that the conductivity measured in a dry N_2 atmosphere could be assumed to be that of pure oxygen ions. We also reported that the proton conductivity in $La_{0.6}Ba_{0.4}InO_{3-\delta}$ was observed in a wet atmosphere but was negligible above 500 °C due to dehydration, which occurred at about 250 °C [14].

Oxygen ion conductivities of the excess Ba-doped $La_{0.6}Ba_{0.4}InO_{3-\delta}$ in the temperature range of 600–1200 °C in a dry N_2 atmosphere are shown in Fig. 1. Except for the undoped composition the oxygen ion conductivity of the excess Ba-doped compositions showed non-linearity in the Arrhenius type conductivities. The curved behavior in the Arrhenius type plot implies that the activation energy is dependent on the temperature. To our knowledge, the curved behavior of the conductivity in $La_{0.6}Ba_{0.4}InO_{3-\delta}$ has not been reported previously. Kakinuma et al. reported the oxygen ion conductivity of the same composition, but they applied a linear fit to the conductivity data measured in the temperature range of 600–1000 °C [18]. Although a linear fit was applied to the oxygen ion conductivity (Ref. [18]) in Fig. 1, the application of polynomial fitting was more appropriate because the raw data also exhibited curved behavior.

The curved behavior of the oxygen ion conductivity has been reported in stabilized zirconia and doped $LaGaO_3$ perovskite oxide, which show superior oxygen ion conductivity [4–7,20]. In the ZrO_2–Y_2O_3 system, Bauerle and Hrizo offered two hypotheses about the curved behavior of the conductivity with the temperature [20]. The first hypothesis assumed vacancy trapping by the dopant ion in the low temperature region, that is, the electrostatic association of oppositely charged defects. The second hypothesis was based on the resistance of the grain boundary layer. It was

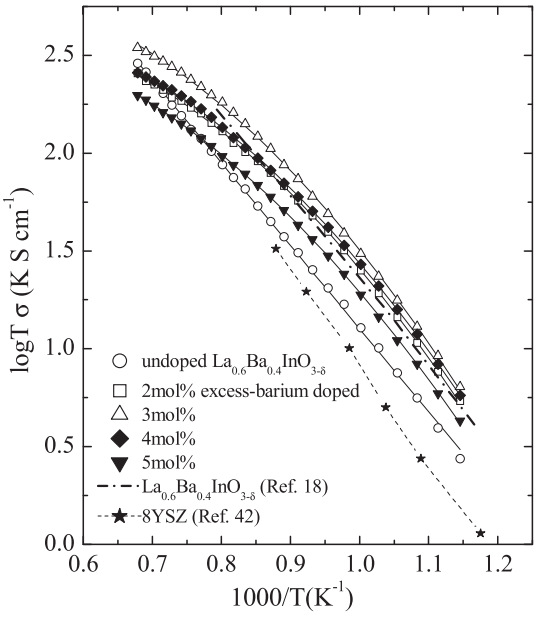

Fig. 1. Arrhenius-type oxygen ion conductivities for undoped and excess Ba-doped $La_{0.6}Ba_{0.4}InO_{3-\delta}$ measured in the temperature range of 600–1200 °C in a dry N_2 atmosphere.

considered that the grain boundaries primarily affect the total conductivity at low and intermediate temperatures (<700 °C) but have little influence at high temperatures [21]. Because the oxygen ion conductivity in this study was measured in the temperature range of 600–1200 °C, the second hypothesis of the grain boundary layer could be discounted.

Moreover, Huang et al. observed curved behavior of the conductivity for a Sr and Mg co-doped $LaGaO_3$ system and suggested that it might be caused by the trapping of oxygen vacancies by the dopant cations below a critical temperature, T* (~600 °C) [4]. The temperature region of 600–850 °C has been treated as the transition region of the conductivity by several researchers, i.e., the difference in activation energy between the high- and the low-temperature regions [5–7]. For doped $LaGaO_3$, the activation energies obtained in the high- and the low-temperature regions have been reported as 0.58–0.82 eV and 0.95–1.20 eV, respectively. Huang et al. also suggested that all oxygen vacancies are mobile above the critical temperature, which implies that the activation energy in the high-temperature region might correspond to the migration energy. In the low-temperature region, the activation energy might be the sum of the migration energy and the association energy due to the coulombic forces between dopant cations of negative defects and oxygen vacancies of positive defects. Therefore, the activation energy for oxygen ion conduction is much higher in the low-temperature region than in the high-temperature one.

In this study, the temperature ranges above and below 900 °C were regarded as the high- and the low-temperature region, respectively. The activation energy values of the high-temperature region, i.e., the migration energy, for the excess Ba-doped compositions were measured as 0.50–0.52 eV, which are slightly lower than the measured values for the doped $LaGaO_3$ system and are similar to the calculated migration energy values of oxygen vacancies for the series of compounds based on the $LaMO_3$ perovskite oxides (M = Cr, Mn, Fe, and Co) showing 0.48–0.61 eV, except for M = Mn calculated as 0.86 eV, as can be seen in Table 1 [22]. Especially, the excess Ba-doped $La_{0.6}Ba_{0.4}InO_{3-\delta}$ show significantly lower activation energy values of both the high- and low-temperature regions compared with YSZ. The oxygen ion conductivity of the 3 mol% excess Ba-doped composition at 800 °C was 5.6×10^{-2} S cm^{-1} as shown in Fig. 1. This value is lower than that of the doped $LaGaO_3$ (>0.1 S cm^{-1}) but much higher than that of YSZ. The low activation energy and relatively high oxygen ion conductivity of $La_{0.6}Ba_{0.4}InO_{3-\delta}$ is discussed below.

Table 1
Activation energy values in the high- and the low-temperature regions for undoped and excess Ba-doped $La_{0.6}Ba_{0.4}InO_{3-\delta}$.

			Activation energy (eV)		Remarks
			High-temperature	Low-temperature	
$La_{0.6}Ba_{0.4}InO_{3-\delta}$					
Undoped			0.84		This study
2 mol% excess Ba-doped			0.51	0.83	This study
3 mol%			0.51	0.87	This study
4 mol%			0.50	0.81	This study
5 mol%			0.52	0.82	This study
$La_{1-x}A_xGa_{1-y}Mg_yO_{3-\delta}$					
A	*x*	*y*			
Ca	0.10	0.20	0.75	1.20	Ref. [7]
Sr	0.10	0.20	0.74	1.08	Ref. [7]
Sr	0.10	0.20	0.66	1.13	Ref. [6]
Sr	0.20	0.15	–	1.06	Ref. [5]
Sr	0.20	0.17	0.82	1.08	Ref. [4]
Ba	0.10	0.20	0.71	0.95	Ref. [7]
$LaMO_3$					
Cr			0.48		Ref. [22]
Mn			0.86		Ref. [22]
Fe			0.50		Ref. [22]
Co			0.61		Ref. [22]
8YSZ			0.91	1.19	Ref. [42]

To understand oxygen ion conduction in perovskite-structured oxides such as $LaGaO_3$ and $LaAlO_3$, where aliovalent cations are substituted at the host ion sites for the formation of oxygen vacancies, several parameters influencing the oxygen ion conductivity and the activation energy have been suggested [23–29]. Among them, the lattice free volume, defined as the difference between the unit cell volume and the total volume occupied by all constituent ions, i.e., $V_f = a_0^3 - 4/3\pi \sum r_i^3$, the Goldschmidt tolerance factor, which is a well-known factor for the stability of the perovskite structure and is defined as $G_t = (r_A + r_O)/(\sqrt{2}(r_B + r_O))$, and the critical radius, defined as the critical size of the triangle formed by two A-site cations and one B-site cation where oxygen ions move into adjacent oxygen vacancies along the <110> edges of the BO_6 octahedra, i.e., $r_c = r_A^2 + 3/4a_0^2 - \sqrt{2}a_0 r_B + r_B^2/2r_A + \sqrt{2}a_0 - 2r_B$, are proposed as the structural parameters.

Sammells et al. found a relationship between the activation energy for ionic migration in perovskite oxides and the lattice free volume, where the activation energy increased as the free volume decreased [23–25]. This relationship might, however, be overestimated because activation energy values for proton conduction as well as oxygen ions were collected in various perovskite oxides including titanate, zirconate and cerate. They pointed out that this criterion could be expanded to the fluorite structure. However, the opposite correlation was observed in this circumstance; the reason was unclear. According to this parameter, moreover, $LaInO_3$ having the largest free volume among Sr and Mg co-doped $LaMO_3$ (M = Al, Ga, Sc, and In) should be the best ionic conductor. However, the oxygen ion conductivity of the doped $LaInO_3$ was slightly lower than that of the doped $LaGaO_3$, with an intermediate free volume value showing the highest oxygen ion conductivity among the samples.

Cook and Sammells proposed that cubic perovskites are only observed for the tolerance factors between 0.95 and 1.04, while the perovskites are stable for $0.75 < G_t < 1.0$ [24]. While the cubic structure is ideal, $G_t = 1$, the majority of perovskite oxides have a distorted structure such as an orthorhombic structure for tolerance factors smaller than 0.90 but larger than 0.75 and hexagonal structures for those larger than 1.0. They also suggested that the cubic structure might be preferred for perovskite solid electrolytes because, in going from orthorhombic to cubic structures, the number of crystallographically equivalent sites increased, which is one of the criteria for achieving high ionic mobility in solid electrolytes. The high crystal symmetry of $La_{0.6}Ba_{0.4}InO_{3-\delta}$, which has a cubic structure, might be correlated to the low migration energy, i.e., the high mobility of oxygen ions.

Mogensen et al. have claimed that the most important parameter controlling the oxygen ion conductivity is the degree of distortion from the fully symmetric and stress free lattice, in which the oxygen ion had the highest mobility and the lowest activation energy for hopping [28]. They defined the stress-free lattice as the ideal perovskite structure, with a cubic closest packing, where the A-site cation should be equal in size to the oxygen ion, $r_A = r_O = 0.14$ nm, and the radius of the ideal B-site cation, $r_{B,Ideal}$, should be 0.058 nm in a defect-free lattice. They stated that La^{3+} (r = 0.136 nm in 12-fold coordination [30]) and Sr^{2+} (0.144 nm) were appropriate A-site ions for maximizing the conductivity, and the ionic radius of Ga^{3+} (0.062 nm in 6-fold coordination) was 9% larger than $r_{B,Ideal}$, whereas Al^{3+} was too small and In^{3+} was too large in the $LaMO_3$ compounds. From the concept of the stress-free lattice, it is considered that a large In^{3+} ion might yield a lattice stress in $LaInO_3$, and this stress can be relaxed by the substitution of

a large Ba^{2+} ion with a small La^{3+} ion, as in this study, resulting in a low migration energy.

Ranlov et al. stated that the critical radius of Mg-doped $LnAlO_3$ (Ln = Er, Gd, Sm, Nd and La) increased with a decrease in the radius of the rare-earth ion, and the conductivity increased with an increase in the critical radius [30]. However, this parameter was not able to be adapted to the entire set of oxygen ion conductors; on the basis of the critical radius, the oxygen ion conductivity of $LaScO_3$ should be higher than that of $LaGaO_3$, and $LaInO_3$ should exhibit the highest oxygen ion conductivity. However, these are calculated values based on the assumption that ions do not behave as immobile hard spheres. As Marques and Kharton point out, ionic polarizability and relaxation from the ideal positions have to be taken into consideration [29]. The polarizability of the lattice depends on the polarizability of the ingoing ions and increases with increasing ionic radius. Indium and barium have relatively large polarizability values (2.81×10^{-3} and 6.40×10^{-3} nm^3, respectively) [31], which may be correlated with high oxygen ion conductivity and low migration energy of $La_{0.6}Ba_{0.4}InO_{3-\delta}$. Meanwhile, the activation energy of $La_{0.9}Sr_{0.1}InO_{3-\delta}$ obtained in the high temperature region of 730–980 °C was 0.70 eV, which is higher than that of $La_{0.6}Ba_{0.4}InO_{3-\delta}$ (ca. 0.50 eV). This suggests that the low polarizability of strontium (4.24×10^{-3} nm^3) is one of the reasons for the high activation energy of $La_{0.9}Sr_{0.1}InO_{3-\delta}$. Consequently, the formation of a cubic structure with a high G_t value, a less stressed lattice due to the substitution of a large Ba^{2+} ion, and the relatively large values of polarizability for indium and barium might yield a low migration energy for oxygen ions in $La_{0.6}Ba_{0.4}InO_{3-\delta}$ and a relatively high oxygen ion conductivity.

On the other hand, it is interesting that there are three types of triangles that oxygen ions pass through in $La_{0.6}Ba_{0.4}InO_{3-\delta}$, La–In–La, La–In–Ba and Ba–In–Ba because 40 at.% of La-sites are substituted by barium, and each triangle might have a different critical radius. The critical radius of the La–In–La triangle (0.1003 nm) was 20% larger than that of the Ba–In–Ba triangle (0.0836 nm), suggesting that less energy might be required to move oxygen into adjacent vacancies through the La–In–La triangle. Further studies about the pathway for oxygen ions in $La_{0.6}Ba_{0.4}InO_{3-\delta}$ are necessary because the larger electrostatic force of the La^{3+} ion compared to the Ba^{2+} ion might result in more difficult movement of oxygen ions through the La–In–La triangle.

The isothermal conductivity as a function of the content of excess Ba is shown in Fig. 2. With the increase in the Ba content, the oxygen ion conductivity increased up to 3 mol% excess and then decreased. The increase in the conductivity might be correlated to the supplementation of Ba^{2+} ions on the vacant A-site, which was caused by the volatilization of Ba during the heat-treatment processes. The volatilization of Ba has been reported in barium cerates and barium zirconates, which are well known proton conductors [32,33].

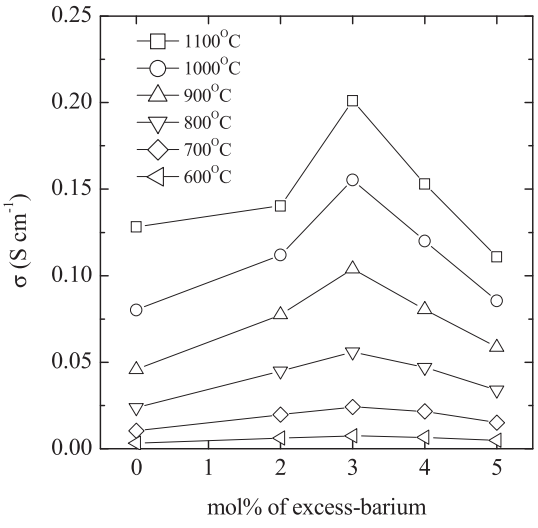

Fig. 2. Isothermal conductivities of $La_{0.6}Ba_{0.4}InO_{3-\delta}$ as a function of excess Ba amount.

Table 2
ICP elemental analysis data for the undoped and excess Ba-doped $La_{0.6}Ba_{0.4}InO_{3-\delta}$.

$La_{0.6}Ba_{0.4}InO_{3-\delta}$	Element stoichiometry (molar ratio)		
	La	Ba	In
Undoped	0.6010	0.3828	1
3 mol% excess Ba-doped	0.6002	0.4167	1

To verify that we had obtained the designed compositions, ICP spectroscopy analysis has been carried out. The results are shown in Table 2. While 3 mol% excess Ba-doped $La_{0.6}Ba_{0.4}InO_{3-\delta}$ sample showed the designed stoichiometric composition, the Ba content of the undoped $La_{0.6}Ba_{0.4}InO_{3-\delta}$ sample is less than 0.4. Based on the elemental analysis of these samples, the volatilization of Ba in $La_{0.6}Ba_{0.4}InO_{3-\delta}$ during high temperature sintering process at 1500 °C could be confirmed.

Through the loss of Ba, A-sites in the ABO_3 perovskite structure became vacant, and the substitution of B-site cations on A-sites occurred. Similar behavior is also expected to occur in the undoped composition due to the linear behavior of the conductivity up to 1200 °C, whereas the other compositions exhibited curved

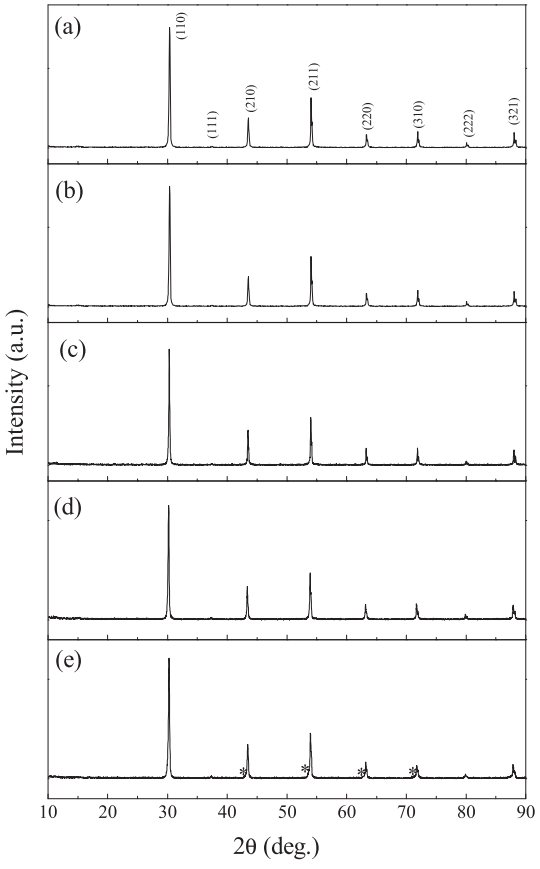

Fig. 3. Powder X-ray diffraction patterns for excess Ba-doped $La_{0.6}Ba_{0.4}InO_{3-\delta}$ at (a) 0 mol%, (b) 2 mol%, (c) 3 mol%, (d) 4 mol%, and (e) 5 mol% excess Ba-doped composition (*unidentified phase).

behaviors, as mentioned above. It is suggested that the substitution of In^{3+} ions on vacant A-sites might cause an association between small In^{3+} ions and oxygen vacancies. On the other hand, the decrease in the oxygen ion conductivity after the maximum value at a 3 mol% doped composition may be correlated with the formation of secondary phases, as shown in Fig. 3. For the 5 mol% doped composition, shoulders were observed on some peaks, indicating that a small amount of barium-containing compound was formed. Other than in the 5 mol% doped composition with secondary phases, however, a single phase of perovskite with a cubic structure was observed in the other compositions. However, based on the maximum point of conductivity being at a 3 mol% composition, it is considered that a small amount of secondary phase might be also formed at the 4 mol% doped composition, although no peaks of the secondary phase were detected by powder X-ray diffraction. Moreover, electrical conductivity is also affected by the microstructure. As shown in Fig. 4, relatively large amount of closed pores were observed in the undoped $La_{0.6}Ba_{0.4}InO_{3-\delta}$ sample, compared with the 3 mol% excess doped composition. This indicates that lower ionic conductivity of the undoped composition than the 3 mol% excess doped composition is also due to rather lower relative density caused by the volatilization of Ba during high temperature sintering process.

3.2. $La_{1-x}Ba_xInO_{3-\delta}$ ($0.4 \leq x \leq 0.8$) system

Powder X-ray diffraction patterns of the 3 mol% excess Ba-doped $La_{1-x}Ba_xInO_{3-\delta}$ ($0.4 \leq x \leq 0.8$) sintered at 1500 °C in air are shown in Fig. 5. A single phase of the perovskite structure was formed in all compositions, and the diffracted pattern could be indexed to a simple cubic structure, indicating that the formation region of the cubic structure in this study was relatively larger than those of previous studies [15,18]. Kakinuma et al. demonstrated that the cubic symmetry was formed from $x = 0.4$ to 0.5, and they also reported that the tetragonal and the orthorhombic structures were formed in the range of $0.5 \leq x < 0.7$ and $0.7 \leq x \leq 1.0$, respectively [18]. Moreover, Tenailleau et al. reported that the cubic structure was obtained in the range of $0.4 \leq x \leq 0.775$, and the composition of $x = 0.8$ was analyzed as the tetragonal using hard mode infrared powder absorption spectroscopy, powder X-ray diffraction, and electron diffraction [15]. The lower limit of the cubic structure was in accord with our results, but the upper limit was not, i.e., the composition of $x = 0.8$. In their study on the crystal structure of $0.5 \leq x \leq 1.0$, on the other hand, Uchimoto et al. reported that the defect perovskite with a disordered cubic structure was observed in the range of $0.5 \leq x \leq 0.8$ according to X-ray diffraction data, and $La_{0.2}Ba_{0.8}InO_{2.6}$, i.e., $x = 0.8$, belonged to a cubic structure with a space group of *Pm3m* by Rietveld analysis [17]. They also reported that the coordination number of In^{3+} continuously decreased up to $x = 0.8$, and then a significant decrease occurred as the amount of Ba^{2+} increased [16]. This result suggested that the composition of $x = 0.8$ showed the cubic structure with the "disordered" perovskite rather than the "ordered" brownmillerite. From these results, the formation of the cubic structure in this system is certain, but the formation region of the cubic structure remains unclear. The chosen heat-treatment process might be one of the reasons for the disagreement of the formed phases and their formation limits. While Tenailleau et al. quenched the samples after sintering at

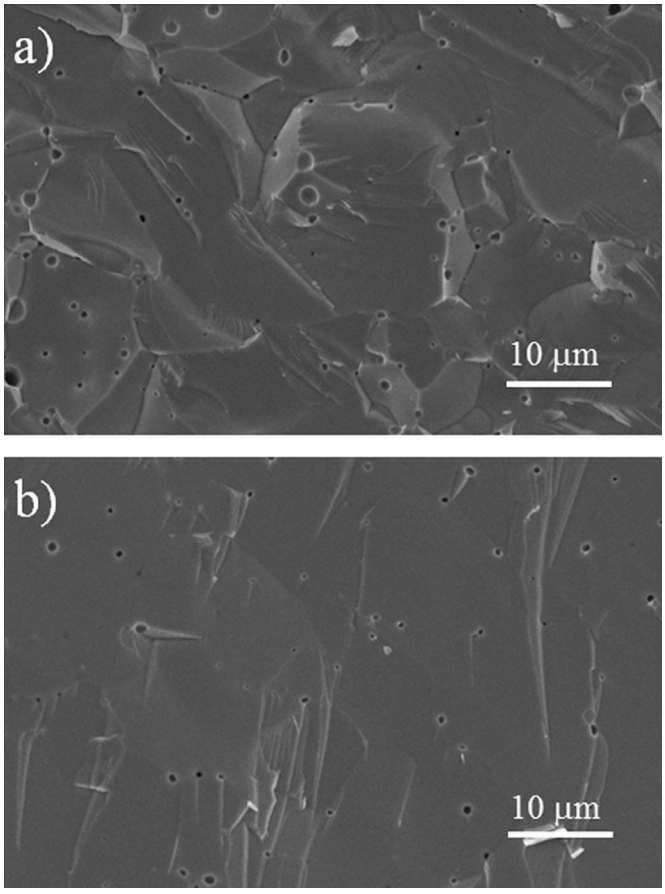

Fig. 4. Fractural surface images of the excess Ba-doped $La_{0.6}Ba_{0.4}InO_{3-\delta}$ at (a) 0 mol% and (b) 3 mol% excess Ba-doped composition, sintered at 1500 °C for 10 h in air.

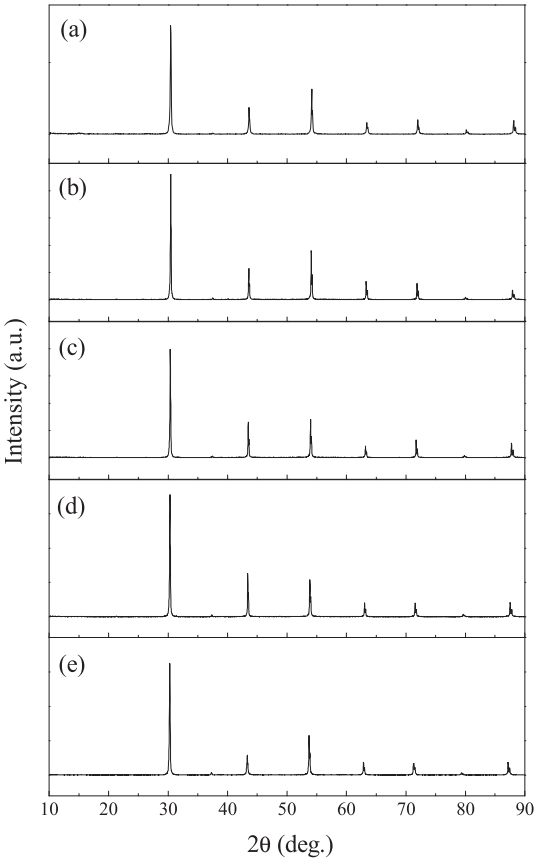

Fig. 5. Powder X-ray diffraction patterns for $La_{1-x}Ba_xInO_{3-\delta}$: (a) $x = 0.4$, (b) $x = 0.5$, (c) $x = 0.6$, (d) $x = 0.7$, and (e) $x = 0.8$.

1300 °C, all the samples in this work were furnace-cooled after sintering at 1500 °C.

$BaInO_{2.5}$ had a brownmillerite structure with an orthorhombic unit cell from room temperature to 900 °C [34]. At 925 °C, a phase transition from orthorhombic to tetragonal structure occurred after a disorder in oxygen vacancies above 900 °C. Then, $BaInO_{2.5}$ became cubic, with an oxygen-deficient perovskite. The formation of the tetragonal structure in the $LaInO_3$–$BaInO_{2.5}$ binary system is reasonable, although the tetragonal structure was not observed in this work, and the phase diagram of the $BaInO_{2.5}$-rich side in this system might be similar to that of the ZrO_2–$YO_{1.5}$ binary system. While ZrO_2 undergoes phase transition from monoclinic to tetragonal and then to cubic with a temperature increase, the cubic structure at high-temperature can be achieved at room temperature by substitution of an Y^{3+} ion on a Zr^{4+}-site [35]. The tetragonal structure obtained by the quenching process as well as the cubic structure achieved after high-temperature sintering, therefore, might be meta-stable phases. This suggestion was supported by the X-ray diffraction pattern of $La_{0.1}Ba_{0.9}InO_{3-\delta}$ ($x = 0.9$), consisting of a mixture of the perovskite with a cubic structure and the brownmillerite with an orthorhombic structure, as shown in Fig. 6. Some diffracted peaks were identified as those of the brownmillerite (ICDD 81-2473), whereas the (200) peak at $2\theta = 29.3°$ and the (341) peak at $2\theta = 51.3°$, which are typical peaks of the brownmillerite, were not observed, suggesting that the peaks with a strong intensity such as $2\theta = 29.9°$, 42.9°, 53.2°, 62.3°, 70.5°, and 86.4° might be those of the cubic perovskite. From the viewpoint of the phase diagram, the formation of a mixture with cubic and orthorhombic structures is reasonable.

The lattice parameter of the cubic structure determined from the powder X-ray diffraction data is shown in Fig. 7. To prevent the incorporation of water into the lattice, the pellets were annealed at 500 °C in a dry N_2 atmosphere using a liquid N_2 trap after the sintering process. In a wet atmosphere, Ba-doped $LaInO_3$ perovskite and $BaInO_{2.5}$ brownmillerite were reported as proton conductors [14,36], and the lattice parameter of the ceramic proton conductors generally became larger under a wet atmosphere due to the incorporation of water vapor into oxygen vacancies [9]. The lattice parameter of the cubic structure showed a non-linear increase as the amount of Ba^{2+} increased. This behavior was also observed in Tenailleau's data [15]. The reason for the non-linearity is not yet clear. It is, however, worth noting the substitution of large Ba^{2+} ions ($r_{Ba} = 0.161$ nm, coordination number = 12 [37]) with small La^{3+} ions ($r_{La} = 0.136$ nm) and the formation of oxygen vacancies smaller than oxygen ions. Through the introduction of large cations, which could preferentially accommodate oxygen ions rather than oxygen vacancies, the anion sub-lattice might be an "ordered" state in a short range order like the brownmillerite structure. Further study is necessary to understand this phenomenon.

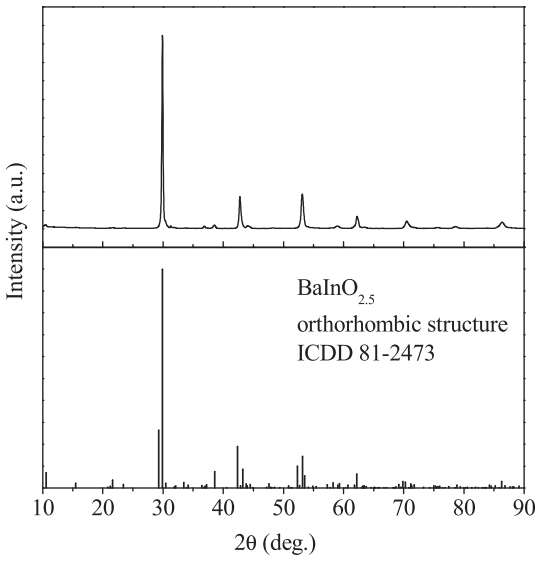

Fig. 6. Powder X-ray diffraction pattern of $La_{0.1}Ba_{0.9}InO_{3-\delta}$.

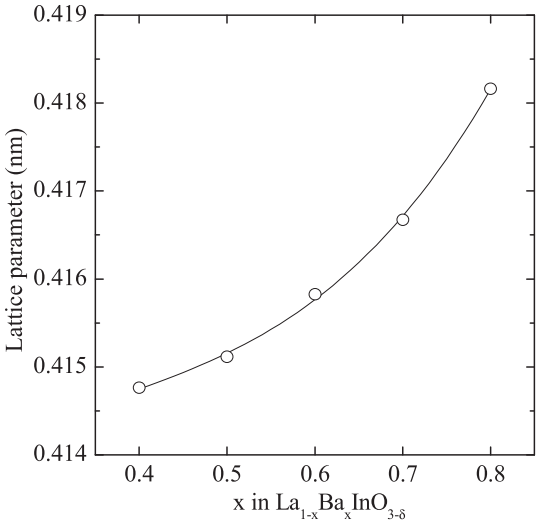

Fig. 7. Lattice parameter of the $La_{1-x}Ba_xInO_{3-\delta}$ system.

In the dry atmosphere, oxides that contain oxygen vacancies are expected to be oxide ion conductors when their electronic conduction is negligible, whereas those exhibiting oxygen ions and electron conduction are expected to be mixed conductors. The conductivity of the mixed conductors consists of the oxide ion conductivity, which is independent of the oxygen partial pressure ($p(O_2)$), and electron/electron–hole conductivities, which are dependent on $p(O_2)$. For a mixed conductor showing oxide ion ($\sigma_{oxygen\text{-}ion}$) and electron hole conductivities ($\sigma_{electron-hole}$), the total conductivity (σ_{total}) is strictly governed by the following equation.

$$\sigma_{total} = \sigma_{oxygen-ion} + \sigma_{electron-hole} = \sigma_{oxygen-ion} + \sigma_P^0 \cdot p(O_2)^a \quad (1)$$

where σ_P^0 and a are the electron–hole conductivity at an oxygen partial pressure of 1 atm and a variable depending on the formation mechanism of electron-holes, respectively. Fig. 8(a) shows the $p(O_2)$ dependence of the DC conductivity of $La_{0.5}Ba_{0.5}InO_{3-\delta}$ at 800 °C measured in dry N_2/O_2 atmospheres using a dry-ice/ethanol trap. By fitting the data using equation (1), $\sigma_{oxygen\text{-}ion}$, σ_P^0, and a were calculated as 4.39×10^{-2} S cm^{-1}, 1.8×10^{-3} S cm^{-1}, and 0.255, i.e., ca. 1/4, respectively. These results indicate that $La_{0.5}Ba_{0.5}InO_{3-\delta}$ might be a mixed conductor of both oxygen ions and electron–holes in the relatively high $p(O_2)$ region of the dry atmosphere. However, $\sigma_{oxygen\text{-}ion}$ was much higher than $\sigma_{electron-hole}$, i.e., the contribution of $\sigma_{electron-hole}$ to σ_{total} is very small even at $p(O_2) = 1$ atm; $\sigma_{p\text{-}type}/\sigma_{total} = 0.04$ and $\sigma_{oxide\text{-}ion}/\sigma_{total} = 0.996$. Therefore, it is reasonable to assume that most of the conducting species in a dry N_2 atmosphere are oxygen ions, and $La_{0.5}Ba_{0.5}InO_{3-\delta}$ is close to a pure oxygen ion conductor even in high $p(O_2)$ region. Meanwhile, because the variable 'a' of Equation (1) was calculated as 0.255, the electron–hole conduction can be considered to occur by the production of electron–holes ($h^{\bullet}$) by dissolution of oxygen into oxygen vacancies ($V^{\bullet\bullet}$), as given in the following equation.

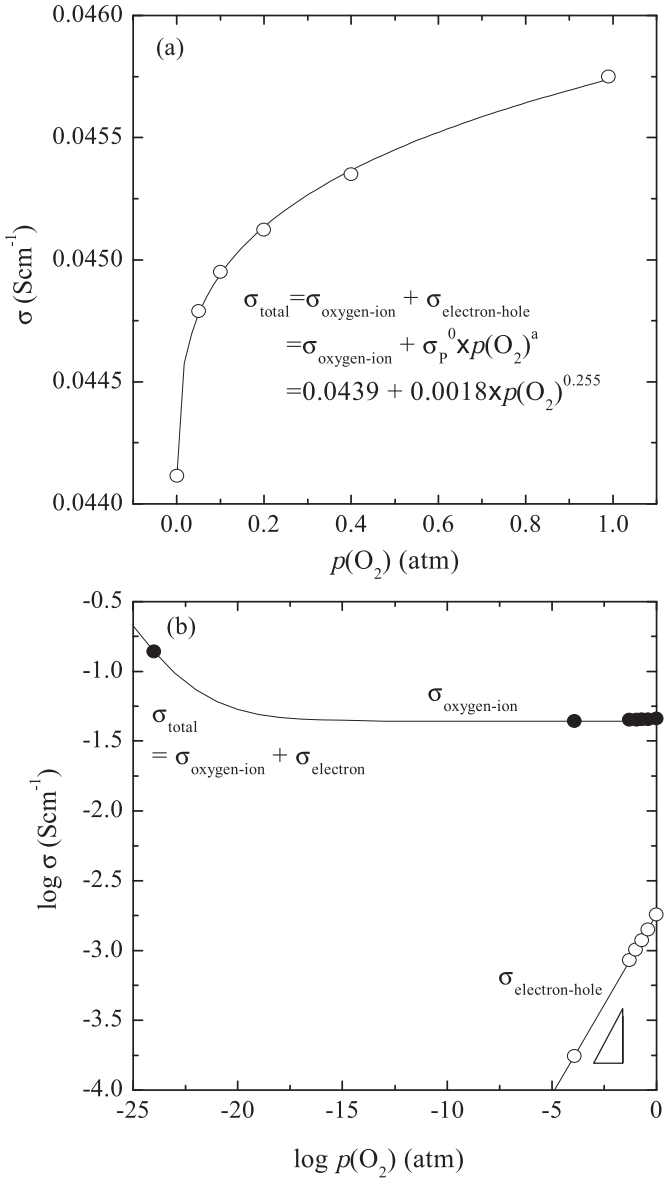

Fig. 8. $p(O_2)$ dependence of conductivity for $La_{0.5}Ba_{0.5}InO_{3-\delta}$ at 800 °C; (a) σ_{total} for high $p(O_2)$ and (b) log σ_{total}, log $\sigma_{oxygen\text{-}ion}$ and log $\sigma_{electron-hole}$ as a function of log $p(O_2)$.

$$1/2O_{2(g)} + V^{\bullet\bullet} = O_O^{\times} + 2h^{\bullet} \quad (2)$$

According to Equation (2), the dependence of electron–hole conductivity (log $\sigma_{electron-hole}$) on oxygen partial pressure [log $p(O_2)$] has a slope of 1/4. The expression of σ_{total} for $La_{0.5}Ba_{0.5}InO_{3-\delta}$ at 800 °C is given by $\sigma_{total} = 4.39 \times 10^{-2} + 1.8 \times 10^{-3} \times p(O_2)^{1/3.92 \approx 1/4}$ S cm^{-1}. The isothermal conductivity including $\sigma_{electron-hole}$ dependent on $p(O_2)$ is shown in Fig. 8(b), where conductivity data was measured in a dry N_2/O_2 mixture gas (~10^{-4} to 1 atm) and a H_2 gas (~10^{-24} atm) using a dry-ice/ethanol trap. The electronic conduction appeared in the low $p(O_2)$ region. Similarly, it has been reported that Sr-doped $LaInO_3$ with an orthorhombic structure showed electronic conductivity in the low $p(O_2)$ region [38], indicating that the electronic conduction in doped $LaInO_3$ is independent of the crystal structure. Further study about the dependence of electronic conductivity on $p(O_2)$ will follow.

Arrhenius type conductivity for $La_{1-x}Ba_xInO_{3-\delta}$ ($0.4 \le x \le 0.7$) measured in the dry N_2 atmosphere is shown in Fig. 9. At 800 °C, the maximum conductivity of 5.6×10^{-2} S cm^{-1} was observed in the compositions of $x = 0.4$. The compositions of $x = 0.6$ and 0.7 showed lower conductivity, although these compositions had a higher concentration of oxygen vacancies. In fact, this behavior of conductivity versus the concentration of the oxygen vacancy has been reported in the literature for oxygen ion conductors [39–41]. The formation of a microdomain with an ordered structure and the associated defect pairs between the dopant cation with the negative effective charge and the charge-compensating oxygen vacancy with the positive effective charge was suggested. The formation of a microdomain might likely occur because, with an increase in x, the amount of Ba in the composition approached the $BaInO_{2.5}$ brownmillerite structure with an ordered oxygen vacancy site. It is, however, noteworthy that the compositions of $x = 0.4$ and 0.5 exhibited curved behaviors of oxygen ion conductivity, and the curvature decreased with increasing x. The composition of $x = 0.7$ exhibited almost linear behavior in conductivity, as shown in Fig. 9, indicating that the activation energy in the high temperature region increased with increase in x. This result suggested that the formation of an association rather than the formation of a microdomain might occur. In the case of the microdomain model, it is expected that the concentration of the carrier decreased, and the activation energy might be unchanged because oxygen ions might migrate freely except in the ordered oxygen vacancy region.

4. Conclusions

Undoped and 2–5 mol% excess Ba-doped $La_{0.6}Ba_{0.4}InO_{3-\delta}$ samples were prepared, and their ion conductivities were measured. The highest conductivity was observed for a 3 mol% excess Ba-doped sample. This is thought to be the result of a Ba-loss phenomenon. The activation energy was dependent on the temperature except in the undoped composition. In the high temperature region above 900 °C, the activation energy was 0.50–0.52 eV, which is slightly lower than that of the doped $LaGaO_3$.

We also investigated the conduction behavior of 3 mol% excess Ba-doped $La_{1-x}Ba_xInO_{3-\delta}$ ($0.4 \le x \le 0.8$) compositions. All of the

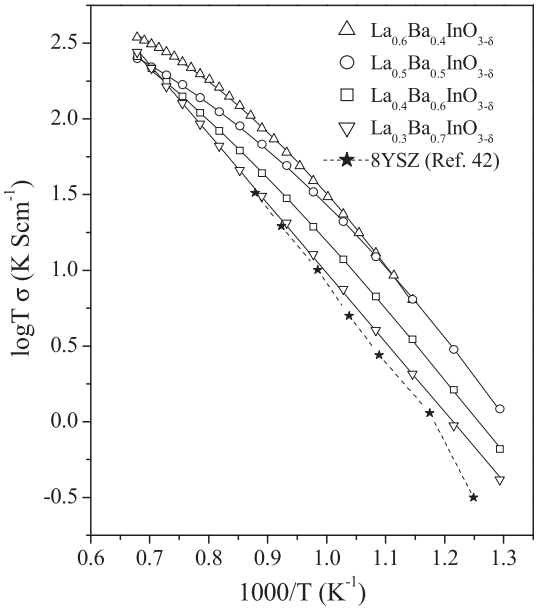

Fig. 9. Arrhenius type oxygen ion conductivities for $La_{1-x}Ba_xInO_{3-\delta}$.

compositions formed a single cubic phase. This is somewhat different than the results reported by other researchers. Lattice parameters increased with increasing Ba concentration due to the larger ionic radius of Ba than La. However, the reason for the non-linear increase in the lattice parameters is unclear.

Electron–hole conduction was dependent on the oxygen partial pressure, while oxygen ion conduction was not. This indicates that $La_{1-x}Ba_xInO_{3-\delta}$ ($0.4 \leq x \leq 0.8$) compositions are nearly pure oxygen ion conductors. The compositions of $x = 4$ and $x = 5$ showed the highest ion conductivity. Although the concentration of oxygen vacancies increased with increasing Ba content, the oxygen ion conductivity decreased. This might be due to the association between dopant cations and oxygen vacancies.

References

[1] T. Takahashi, H. Iwahara, Energy Convers. 11 (1971) 105–111.
[2] J.A. Kilner, R.J. Brook, Solid State Ionics 6 (1982) 237–252.
[3] T. Ishihara, H. Matsuda, Y. Takita, J. Am. Chem. Soc. 116 (1994) 3801–3803.
[4] K. Huang, R.S. Tichy, J.B. Goodenough, J. Am. Ceram. Soc. 81 (1998) 2565–2575.
[5] P. Huang, A. Petric, J. Electrochem. Soc. 143 (1996) 1644–1648.
[6] J. Drennan, V. Zelizko, D. Hay, F.T. Ciacchi, S. Rajendran, S.P.S. Badwal, J. Mater. Chem. 7 (1997) 79–83.
[7] J.W. Stevenson, T.R. Armstrong, D.E. McCready, L.R. Pederson, W.J. Weber, J. Electrochem. Soc. 144 (1997) 3613–3620.
[8] T. Ishihara, Bull. Chem. Soc. Jpn. 79 (2006) 1155–1166.
[9] S. Kim, K.H. Lee, H.L. Lee, Solid State Ionics 144 (2001) 109–115.
[10] K.H. Lee, H.L. Kim, S. Kim, H.L. Lee, Jpn. J. Appl. Phys. 44 (2005) 5025–5029.
[11] E. Ruiz-Trejo, J.A. Kilner, Solid State Ionics 97 (1997) 529–534.
[12] K. Nomura, T. Takeuchi, S. Tanase, H. Kageyama, K. Tanimoto, Y. Miyazaki, Solid State Ionics 154-155 (2002) 647–652.
[13] H.L. Kim, Materials Design and Electrical Properties of LaInO3-Based Perovskite Oxides (Ph. D. Thesis), Yonsei University, Seoul, Korea, 2006.
[14] H.L. Kim, K.H. Lee, S. Kim, H.L. Lee, Jpn. J. Appl. Phys. 45 (2006) 872–874.
[15] C. Tenailleau, A. Pring, S.M. Moussa, Y. Liu, R.L. Withers, S. Tarantino, M. Zhang, M.A. Carpenter, J. Solid State Chem. 178 (2005) 882–891.
[16] Y. Uchimoto, T. Yao, H. Takagi, T. Inagaki, H. Yoshida, Electrochemistry 68 (2000) 531–533.
[17] Y. Uchimoto, H. Takagi, T. Yao, N. Ozawa, T. Inagaki, H. Yoshida, J. Synchrotron Rad. 8 (2001) 857–859.
[18] K. Kakinuma, H. Yamamura, H. Haneda, T. Atake, Solid State Ionics 140 (2001) 301–306.
[19] P. Babilo, T. Uda, S.M. Haile, J. Mater. Res. 22 (2007) 1322–1330.
[20] J.E. Bauerle, J. Hrizo, J. Phys. Chem. Sol. 30 (1969) 565–570.
[21] N.Q. Minh, J. Am. Ceram. Soc. 76 (1993) 563–588.
[22] M. Cherry, M.S. Islam, C.R.A. Catlow, J. Solid State Chem. 118 (1995) 125–132.
[23] R.L. Cook, J.J. Osborne, J.H. White, R.C. MacDuff, A.F. Sammells, J. Electrochem. Soc. 139 (1992) L19–L20.
[24] R.L. Cook, A.F. Sammells, Solid State Ionics 45 (1991) 311–321.
[25] A.F. Sammells, R.L. Cook, J.H. White, J.J. Osborne, R.C. MacDuff, Solid State Ionics 52 (1992) 111–123.
[26] H. Hayashi, H. Inaba, M. Matsuyama, N.G. Lan, M. Dokiya, H. Tagawa, Solid State Ionics 122 (1999) 1–15.
[27] D. Lybye, F.W. Poulsen, M. Mogensen, Solid State Ionics 128 (2000) 91–103.
[28] M. Mogensen, D. Lybye, N. Bonanos, P.V. Hendriksen, F.W. Poulsen, Solid State Ionics 174 (2004) 279–286.
[29] F.M.B. Marques, V.V. Kharton, Ionics 11 (2005) 321–326.
[30] R.D. Shannon, Acta Crystallogr. A32 (1976) 751–767.
[31] J. Ranlov, N. Bonanos, F.W. Poulsen, M. Mogensen, Solid State Phenom. 39-40 (1994) 219–222.
[32] N.W. Grimes, R.W. Grimes, J. Phys. Condens. Matter 10 (1998) 3029–3034.
[33] D. Shima, S.M. Haile, Solid State Ionics 97 (1997) 443–455.
[34] J. Wu, L.P. Li, W.T.P. Espinosa, S.M. Haile, J. Mater. Res. 19 (2004) 2366–2376.
[35] S.A. Speakman, J.W. Richardson, B.J. Mitchell, S.T. Misture, Solid State Ionics 149 (2002) 247–259.
[36] H.G. Scott, J. Mater. Sci. 10 (1975) 1527–1535.
[37] G.B. Zhang, D.M. Smyth, Solid State Ionics 82 (1995) 153–160.
[38] H. He, X. Huang, L. Chen, Electrochim. Acta 46 (2001) 2871–2877.
[39] T.H. Etsell, S.N. Flengas, Chem. Rev. 70 (1970) 339–376.
[40] J.A. Kilner, Solid State Ionics 129 (2000) 13–23.
[41] J. Faber, C. Geoffroy, A. Roux, A. Sylvestre, P. Abelard, Appl. Phys. A 49 (1989) 225–232.
[42] Y. Li, J. .Gong, Y. Xie, Y. .Chen, J. Mater. Sci. Lett. 21 (2002) 157–159.